DUFED, 3(1), 79 - 86, 2014

Sprey metodu ile hazırlanmış çinko oksit filmlerinin özelliklerinin incelenmesi: Optik ve dielektrik parmetreler

Mostefa Benhaliliba

Technology of Material Department, Physics Faculty, Oran University of Sciences and Technology USTOMB, BP1505 Oran, Algeria.

Özet

Bu makalede FTO alttaşları üzerine sprey proliz yöntemi ile büyütülmüş çinko oksit ince filmlerinin optik ve dielektrik parametreleri üzerine katkı ve tavlama koşullarının etkisi sunulmuştur. Büyütülen filmler saf, alüminyum katkılı (AZO) ve indiyum katkılı (IZO) çinko oksit (ZnO) şeklindedir. Film kalınlıkları ise yaklaşık 150 nm (ZnO) ve 1 µm (AZO ve IZO) kadardır. 400 ^{O}C de 1 saat hava ortamında tavlanmış ve tavlanmamış ZnO AZO ve IZO ince filmlerin geçirgenlik ve yansıma özellikleri incelendi. Dielektrik parametreler ise Didomenico ve Wemple yarı ampirik model ile uyumlu olarak kırıcılık indisi bağıntısı ile elde edildi. Yük taşıyıcı konsantrasyonu n_c 19x10^{19} ile 55 10^{19} cm^{-3} aralığında ve optik band aralığı (Eg) 3.20 ile 3.29 eV aralığındadır. Yüksek frekans indisi 1.19 ile 2.38 ve osilatör gücü (S_0) 2 10^{12} ile 46.7 10^{12} m^{-2} aralığındadır.

Anahtar Kelimeler: Yansıma; geçirgenlik; dielektrik sabit; kırılma indisi; enerji dağılımı; ZnO; AZO; IZO

The study of the sprayed zinc oxide films properties: optical and dielectric parameters

Abstract

In this paper, we present the doping and the annealing effect on the optical and dielectric parameters of spray pyrolyzed zinc oxide thin films grown onto the FTO substrates. Our as-grown films are pure, aluminium (AZO) and indium (IZO) doped ZnO. The film thicknesses were about 150 nm (ZnO) and 1µm (AZO and IZO). The transmittance and reflectance of ZnO, AZO and IZO thin films as grown and annealed at 400 ^{O}C for one hour in air were investigated. The dielectric parameters are deduced from the refractive index relation in accordance with the Didomenico and Wemple semi-empirical model. The charge carrier concentration n_e ranged within the range 19 10^{19} to 55 10^{19} cm^{-3}, optical band gap Eg varied from 3.20 to 3.29 eV. The high frequency index goes from 1.17 to 2.38 and the oscillator strength S_0 from 2 10^{12} to 46.7 10^{12} m^{-2}.

Anahtar Kelimeler: reflectance; transmittance; dielectric constant; refractive index; dispersive energy; ZnO; AZO; IZO.

Corresponding author: (e-mail: mbenhaliliba@gmail.com)

1. Introduction

The technical importance of transparent zinc oxide (ZnO) thin films has encouraged many studies of its electrical, optical, compositional, and structural characteristics. As a wide band gap (>3.4 eV) semiconductor, ZnO is one of the most investigated and used material since last decade. ZnO has a stable wurtzite structure with the following lattice parameters $a = 3.25$, $c = 5.21$ Å. It has attracted intensive research effort for its unique properties and multitalented applications in transparent electrodes [1], ultraviolet (UV) light emitters [2], gas sensors [3], optical devices [4], solar cell applications [5], spinotronics [6]. Invisible thin film transistors (TFT s) using ZnO as an active channel have achieved much higher field effect mobility than amorphous silicon TFT s. These transistors can be widely used for display applications. ZnO has been proposed to be a more promising UV emitting phosphor than GaN because of its larger exciton binding energy (60 meV). This leads to a reduced UV lasing threshold and yields a higher UV emitting efficiency at room temperature. We have showed a large study of optical and dielectric properties of ZnO, AZO and IZO before and after annealing process. From the Didomenico and Wemple semi-empirical model [7, 8], some parameters are obtained such as the energies E_0, Ed which were the average excitation energy for electronic transitions and the dispersion energy, respectively.

2. Experimental procedure

Zinc acetate dehydrated, Zn $(CH_3COO)._2(H_2O)_2$ was the starting material used for the solution preparation. The homogenous and clear solution was then sprayed during 5 mn using ultrasonic nebulizer system onto fluorine tin oxide (FTO) glass coated substrate, of sheet resistance 15Ω/sq, supplied by Pilkington Group Ltd. as mentioned in earlier reports [ ]. The zinc acetate concentration was 0.1 M and the doping ratio Al/Zn, In /Zn were 2% in the solution. Films were annealed at 400 °C for one hour in air. The optical parameters were measured using a double beam spectrophotometer Shimadzu UV-3101PC [9].

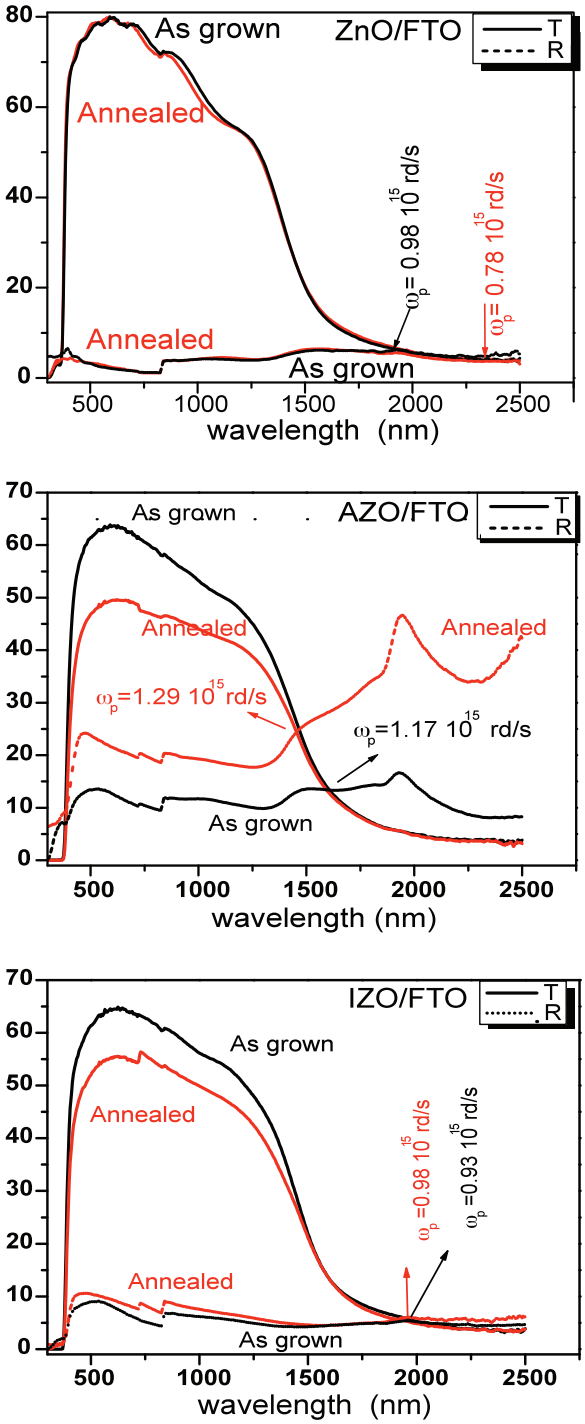

Figure 1. *The plot of transmittance and reflectance of the as-grown and annealed ZnO (a), AZO (b), IZO (c) films.*

Table 1. *The plasma frequency, the electron density, the optical band gap and their corresponding wavelength of the as-grown and the annealed undoped and doped ZnO films.*

Material	ω_p (10^{15} rd/s)		n_e (10^{19} cm^{-3})		E_g (eV)		λ (nm)	
	As grown	**Annealed**	**As grown**	**Annealed**	**As grown**	**Annealed**	**As grown**	**Annealed**
ZnO	0.98	0.78	31.36	19,87	3.28	3.29	377.78	378.58
AZO	1.17	1.29	44.70	54.35	3.26	3.27	380.21	379.28
IZO	0.93	0.98	28.24	31.36	3.29	3.20	377.55	387.93

3. Results and discussion

The *figure 1* depicts the transmittance and the reflectance of ZnO, AZO and IZO thin films as grown and annealed. From the intersection of transmittance and reflectance curves we deduced the plasma cut off frequency ...p (expression 1), ε_r=8.3 is the dielectric parameter and the mass ratio (m^*/m_e) is 0.28 for zinc oxide,

$$\omega_p = \left(\frac{ne^2}{m^* \varepsilon_0 \varepsilon_r}\right)^{1/2} \quad (1)$$

Where m* is the electron effective mass, we determine then the effective carrier concentration ne from the relation 1 and the data were listed in *table 1*

The annealing increased strongly the reflectance of the AZO films near the tail band around 2000 nm as sketched in *figure 1*(b), and a strong peak of reflectance is observed, while the effect was nearly unremarkable in our IZO films and no change was distinctly observed for the pure zinc oxide. Both the doping and the annealing decreased the transmittance as can be seen in *figures 1* b and c. As shown in *figure 1*, the transmittance intercepts the reflectance in IR band, this fact is obviously evidenced in both AZO and IZO samples.

From the optical measurements shown in *figure 2*, we calculated the optical band gap of our films and their corresponding wavelength; these values are reported in *Table 1*. We assessed the accuracy of the calculated optical band gap, following the expression ($E_{g\ as\ grown}$ $E_{g\ annealed}$ /$E_{g\ as\ grown}$) as being 0.21%, 0.37% and 2.68%, for ZnO, AZO and IZO thin films, respectively. It is evident that the annealing has a little effect on the optical band gap in ZnO and AZO films, while the indium doping has a strong narrowing effect. The optical band gap, E_g, was calculated from the best fit of the plot $(\alpha h\nu)^2$ versus the incident photon energy hv, and the extrapolation of its linear part to $(\alpha h\nu)^2$ =0, as can be observed in *figure 2*. The extinction coefficient, k, was obtained by using the following relation,

$$k = \frac{\alpha\lambda}{4\pi} \quad (2)$$

Where α is the absorption coefficient and λ is the photon wavelength. The refractive index dispersion for the energies less than optical gap (E_g ~3.27eV) was analyzed by the single oscillator model which developed by Didomenico and Wemple [7, 8]. Defining two parameters, the oscillation energy, E_0, and the dispersion energy, E_d, the model concludes [10]:

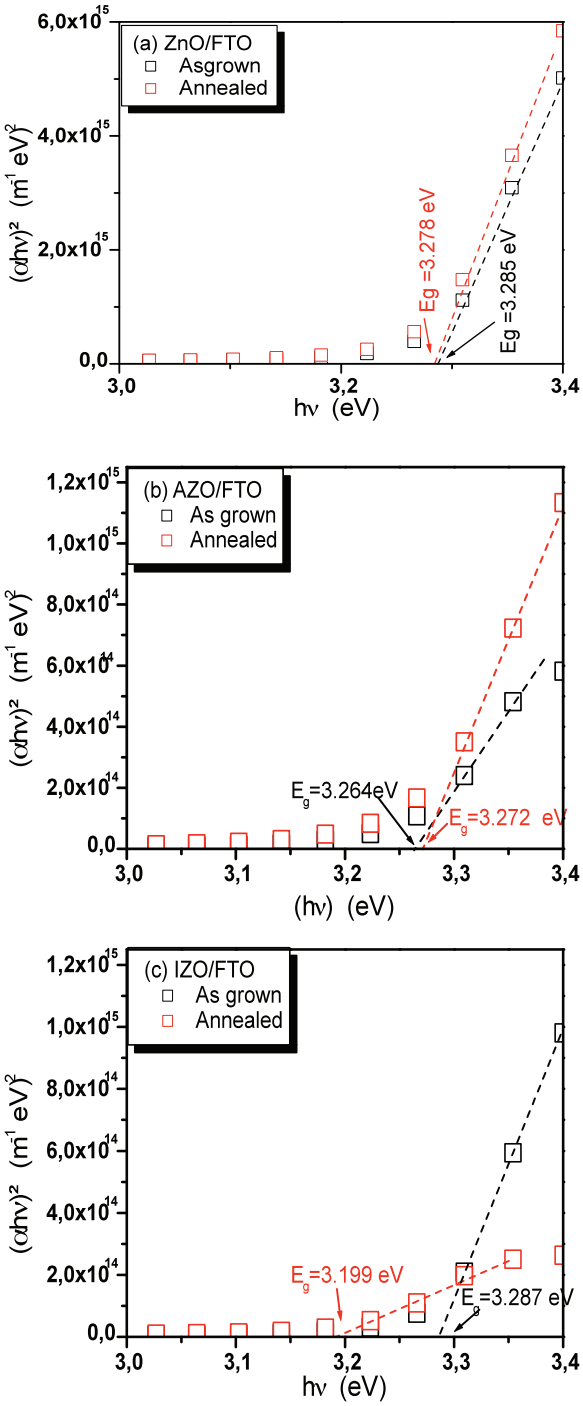

Figure 2. The variation of (±hΩ)≤ versus photon energy (hΩ) of the as-grown and annealed ZnO (a), AZO (b), IZO (c) films.

$$\frac{1}{n^2-1}=\frac{E_0^2-(h\nu)^2}{E_d E_0} \qquad (3)$$

Both Wemple parameters can be obtained from the slope and the intercept with the Y axis of the plot $(n^2\text{-}1)^{-1}$ against E^2. The ***figure 3*** displays the refractive index, n, versus wavelength, for ZnO (a), AZO (b) and IZO (c). In the visible range (400-700 nm), the annealing has a little effect on the refractive index of the sprayed ZnO film. The annealing effect was important for the AZO and IZO as it can be seen in ***figures 3*** (b) and (c) respectively. As shown in these figures, it becomes evident that nature of doping has a pronounced effect on the refractive index. By the annealing, it improves further, but its final value seems to be less doping-dependent. May be this could be attributed to the crystal structure improvement after the annealing procedure. The refractive index was found to increase after Al, In incorporation in ZnO. Around 400 nm (3.1 eV), a high peak is exhibited for the as-deposited ZnO film, which it is reduced by the thermal annealing. An important decay is then followed for both as-deposited and annealed films in the range 600-800 nm. It is revealed that the high peak is broadened and shifted to the larger wavelength for both AZO and IZO cases. Here, the thermal annealing has improved the refractive index; this can be explained by the crystalline structure and the reflectance improvement. Al doping level decreases slightly the transmittance and the optical band gap, while it increases the refractive index, this is also reported by Oriaku [11]. From the plot $(1/n^2\text{-}1)$ versus $(hv)^2$, we determine, for $(hv)^2=0$, the ratio E_0/E_d and the value of E_d is then found from the slope of the linear fit as seen in fig.4.

The dependence of the refractive index on the reflectance R and the extinction coefficient k was expressed as follows [12],

$$n=\frac{1+R}{1-R}+\sqrt{\frac{4R}{(1-R)^2}-k^2} \qquad (4)$$

Where k, depends on photon wavelength λ and absorption α, was given by relation 2.

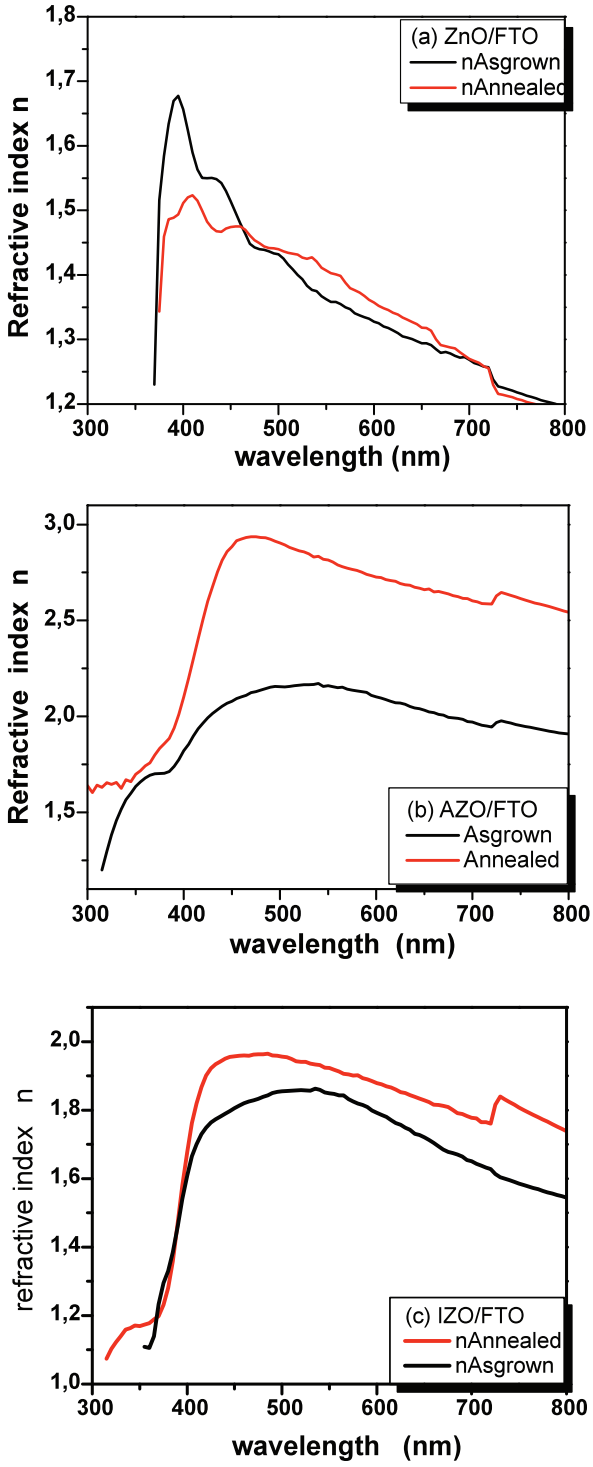

Figure 3. *The refractive index plot of ZnO, AZO and IZO (as-grown and annealed) films.*

In according to fit equation, the data deduced are listed in ***table 2***. By plotting the variation of $(n^2\text{-}1)^{-1}$ versus λ^{-2} and then the slope and the calculated ordinate at zero, we deduced the parameters n_∞, λ_0 and S_0 which are expressed by the following relations,

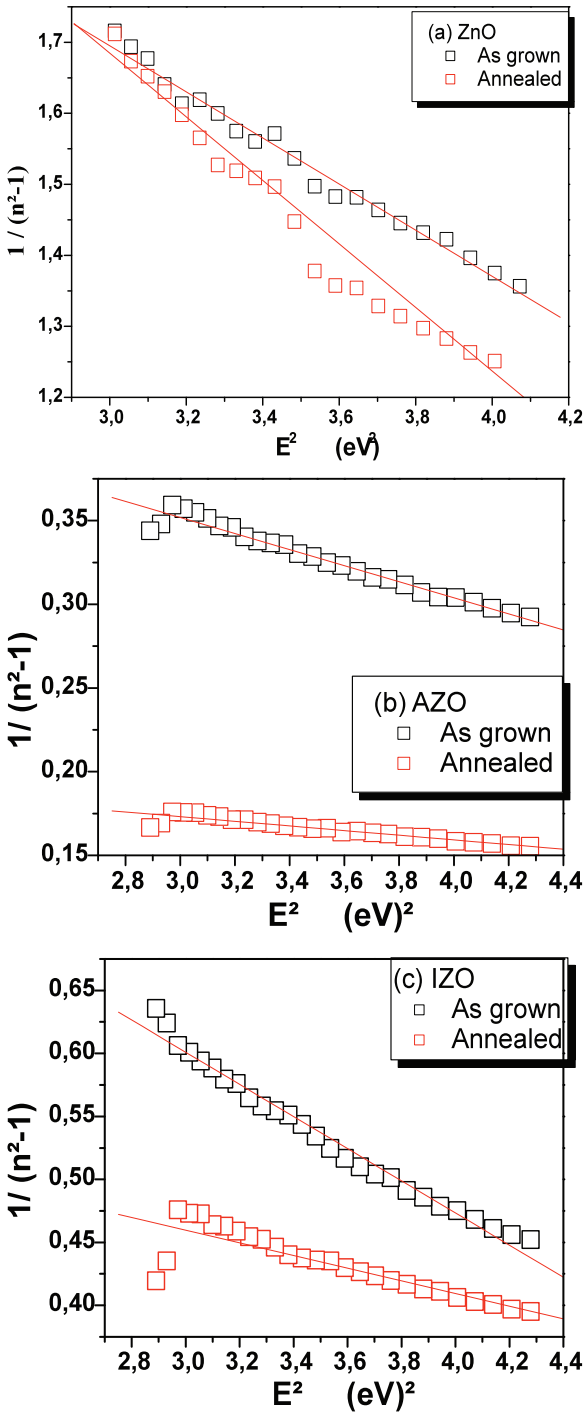

Figure 4. The variation of 1/(n≤-1) versus photon energy of the as-grown and annealed films, the curves were linearly fitted.

$$n^2 - 1 = \frac{n_\infty^2 - 1}{1 - (\frac{\lambda_0}{\lambda})^2} = \frac{S_0 \lambda_0^2}{1 - (\frac{\lambda_0}{\lambda})^2} \qquad (5)$$

And the strength parameter is expressed as follows,

$$S_0 = \frac{n_\infty^2 - 1}{\lambda_0^2} \qquad (6)$$

The dependence of the parameter $1/(n^2\text{-}1)$ on the square of incident photon energy E^2 is plotted in the ***figure 4***. These curves were linearly fitted and the energies E_0 and E_d were then easily extracted, the obtained values are gathered in the ***table 2***. The average excitation energy is ranged within 2.55-3.93 eV and the dispersion energy varied between 0.82 and 18.29 eV. E_0 and E_d values agree fairly well with those reported by Wemple and Caglar [8, 13]. The dispersion energy measures the average strength of interband optical transitions. Wemple and Di Domenico have related this parameter with the coordination number for anion and the valence electrons number per anion. In our case the E_d values increase with Al incorporation relative percentage in the films as listed in ***table 2***.

Furthermore, according to equations 5 and 6, the high frequency index n_∞, the wavelength λ_0 and oscillator strength S_0 were determined from the slope and the intercept of the variation of $(n^2\text{-}1)^{-1}$ versus λ^{-2}, and results are summarized in table 2.

Evolution with photon energy of the real component, ε_1, of the dielectric constant is

Table 2. The average excitation and the dispersion energy, the dielectric parameters of as-grown and annealed ZnO films.

Material	ZnO		AZO		IZO	
	As grown	Annealed	As grown	Annealed	As grown	Annealed
E_0 (eV)	2.87	2.55	3.21	3.93	2.78	3.48
E_d (eV)	1.07	0.82	6.47	18.29	2.82	5.70
High frequency index n_∞	1.17	1.15	1.74	2.38	1.42	1.62
λ_0 (nm)	432.75	485.52	388.33	315.5	447.1	356.28
Oscillator strength S_0 ($10^{12}m^{-2}$)	2	1.36	13.5	46.7	5.1	12.9

depicted in the ***figure 5***. As it can be seen, thermal annealing and doping enhanced the real component of dielectric constant. For ZnO, at optical band gap E_g, the intensity of ε_1 was found to be 1.97 (annealed sample) and negative -3.09 (as grown sample) [14], here we remarked that n is less than k, this is due to absorption around E_g was greater than reflectance, indeed the electron density increased and the annealing decreased it for the undoped case (see table 1). In VIS range, the coefficient k was so weak, then the dielectric constant became $\varepsilon_1 \sim n^2$, in IR and UV range, n takes very low value. Negative constant ε_1 is found for the pure and doped zinc oxide in the very close-fitting photon energy range as can be seen in ***figure 5***. The dielectric constant was given by the following expression,

$$\varepsilon = \varepsilon_1 + i\varepsilon_2 \qquad (7)$$

Where the real ε_1 and the imaginary ε_2 components s of the dielectric constant were determined using the formula $\varepsilon_1=n^2-k^2$ and $\varepsilon_2=2nk$, [15].

In the visible range this evolution is conditioned by the proximity of resonance which be positioned in the UV range. When the frequency goes from red to blue, the dipole moment, p=ex, e is the electron charge, x is the distance between charges, induced by the electrical field E associated with the wave and the polarization, $P=np$ and $P = \varepsilon_0\chi E = \varepsilon_0 (\varepsilon_r -1)E$, of each atom will increase as x increases gradually as the frequency approaches the resonance, the microscopic rise of p explains the macroscopic increase of ε ($\varepsilon_{1\,red} \sim 0.45$, $\varepsilon_{1\,blue} \sim 1.69$ for the as-deposited ZnO) and therefore n which leads to a slightly higher index for blue (n~1.48 for as deposited ZnO) than red (n~1.23 for as deposited ZnO) and thus the decomposition of light by transparent prisms.

In the considered spectral range, the frequency of the incident wave is so high that the electrons can no longer follow the rapid variations of the field, the dipoles that each electron with the ion is still have a direction opposite to the electric field due to the delay of the electrons (in contrast to the situation encountered in electrostatics of dielectrics). The following relation remains valid $\mathbf{D = \varepsilon_0 E + P}$, $\mathbf{P = Np}$, but p and E are non-parallels, then the dielectric susceptibility χ is negative.

When $\omega < \omega_p$: The amplitude of the oscillation of electrons is so large that P is greater than E that to say $\chi < -1$.

When $\omega > \omega_p$: electrons do not always follow field reversals and their elongation is antiphase with E but is lower that previously: $-1 < \chi < 0$. A similar explanation applies to the situation of ions in the infrared between ω_T and ω_L beyond the resonance of lattice ions. In UV range, it still identifies local field and the applied field and the described behavior extends to atomic electrons when it reaches the X rays spectral. ε_2 must necessarily be positive because it describes the energy dissipation associated with the damped wave . The same remarks apply to the energy loss function which is always positive and equal to $\varepsilon_2 / (\varepsilon^2_1 + \varepsilon^2_2)$ but may also be written (±) Im $(1/\varepsilon)$. These remarks concern also $n \pm ik$ where k is necessarily positive (and leads to attenuation).

AZO revealed a red light refractive index found to be 1.97 (as-deposited) and 2.65 (annealed) respectively, while for a blue light AZO exhibits $n_{\text{as deposited}} \sim 2.1$, and $n_{\text{annealed}} \sim 2.93$. Finally, IZO exhibited a refractive index n, for the red light, ~1.60 (as deposited), ~1.83 (annealed), for the blue light ~1.82 (as deposited), ~1.95 (annealed) .

It is obvious, that to state the dielectric constant ε more carefully than is possible under the Lorentz model [16], a more accurate summation of all electronic possible transitions weighted by the corresponding oscillator forces would be needed. This approach would complicate the results without a change in the physical mechanism description.

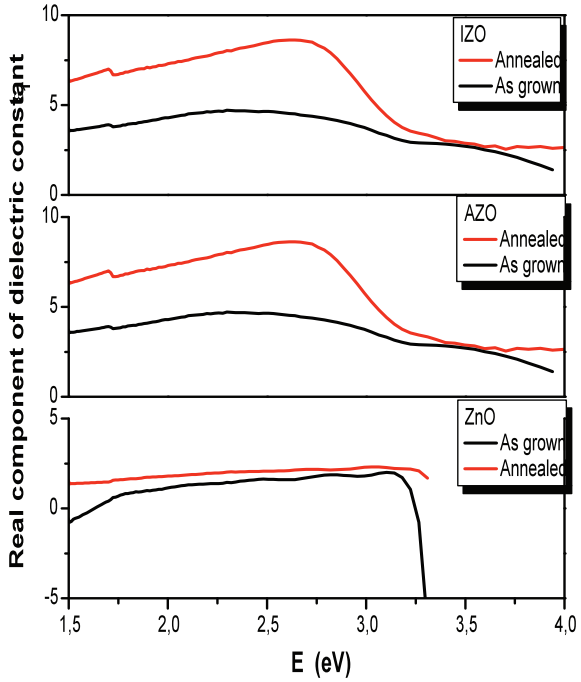

Figure 5. *The plot of the real component μ1 of the dielectric parameter versus the photon energy.*

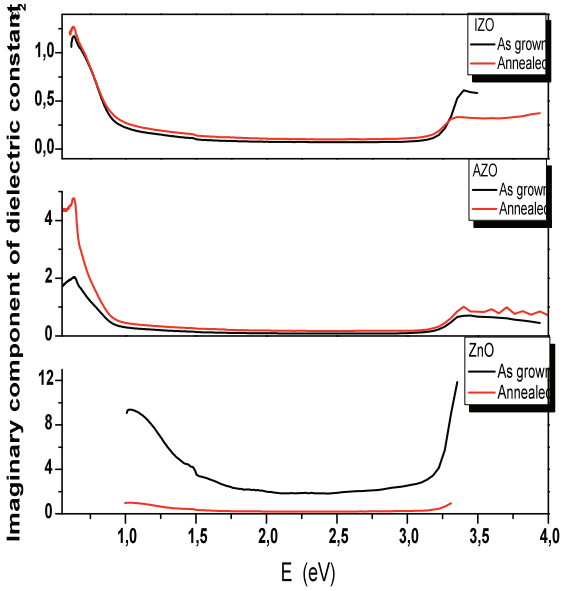

Figure 6. *The plot of the imaginary component μ2 of the dielectric parameter versus the photon energy.*

The variation of the imaginary part ε_2 of the dielectric constant against the photon energy is depicted in the ***figure 6***. It followed approximatively the same profile in ZnO, AZO and IZO. The curve depicts a maximum for the low photon energy (IR domain), a very slow decay followed in VIS area, and then a slight rise reached in UV range in agreement with result found by Caglar [12]. In visible range, μ2 varied slightly and annealing did not change it greatly, except the case of ZnO, where ε_2 decreased noticeably after the thermal annealing. It takes values of 2.5 and 2.23 respectively for blue and red light for as grown ZnO, whereas the annealed film exhibits very slight ε_2. AZO film revealed the same value which is 0.18 for both blue and red frequency, and 0.1 and 0.08 for the red and blue frequency are obtained for IZO film. The figures 5 and 6 revealed that the real component is higher than the imaginary component for doped films; it seems that the optical and dielectric follow the same outline. We remarked that annealing had an important effect on optical and dielectric parameters as shown in figures.

Determination of optical constants of ZnO layers

The refractive index (n) plays a very important role in optical communication and designing of the optical devices. One of the methods for calculating the refractive index (n) is by using the reflectance (R) and the extinction coefficient (k), where $k=\alpha\lambda/4\pi$, of films [45]:

$$n = \left(\frac{1+R}{1-R}\right) + \sqrt{\frac{4R}{(1-R)^2} - k^2} \qquad (8)$$

where n is the real part of the complex refractive index given by. Fig. 7(a) shows the refractive index distributions of pure CdO and Co-doped CdO thin films. The n values decrease rapidly with increasing the wavelength from 350 nm to 500 nm, and then decrease slightly with λ. The n value of undoped CdO film is about 1.7 in most of the visible region of the spectra. Such behavior and value of n is similar to that reported by K. Gurumurugan et al. [17]. Also, the n values of CdO films increase, as shown in the inset of Fig. 7(a), with increasing Co content. This indicates the increase of film density due to the increase in the film thickness (see table 1) with Co content. It has been concluded that when the incident light interacts with a material has a large amount of particles, the refraction will be high and hence the refractivity of the films will be increased.

Conclusion

In the present work, ZnO thin films of different thicknesses have been prepared by an economical and simple spray pyrolysis technique onto FTO substrate at 300 °C from an aqueous zinc acetate solution. The films are then annealed at 400 °C, and show direct band gap in the range 3.20 - 3.29 eV. The films exhibit low absorbance in the visible / near infrared region from ~ 450 nm to 1000 nm. Variations in the optical constants with wavelength are found to be thickness and doping dependent of the films. The optical properties such as refractive index, optical band gap and low dielectric constant of the as-deposited and annealed films show the suitability of the deposited films for using them in optoelectronic devices and solar cells. In conclusion, we can state that the spray pyrolysis deposition could be employed for large-scale synthesis because of its high yield and purity, simple reaction mechanism, simple equipment and relatively low deposition temperature. Therefore, annealing and doping change the optical and dielectric parameters of zinc oxide.

Acknowledgements

This work is included in C.N.E.P.R.U. project supported by the Algerian High Level Teaching and Scientific Research Ministry and Oran Sciences and Technology University USTOMB, under the code **D 01920120039.**

References

[1] Y. Ohya, M. Ueda, Y. Takahashi, Jpn. J. Appl. Phys. 35 (1996) 4738.

[2] D.C. Look, D.C. Reynolds, C.W. Litton, R.L. Jones, D.B. Eason, G. Cantwell, Appl. Phys. Lett. 81 (2002) 1830.

[3] X. Wang, W.P. Careg, S. Yee, Sensors Actuators B 28 (1995) 63.

[4] P.D. Yang, H.Q. Yan, S. Mao, R. Russo, J. Johnson, R. Saykally, N. Morris, J. Pham, R. He, H.J. Choi, Adv. Funct. Mater. 12 (2002) 323.

[5] J. Lee, D. Lee, D. Lim, K. Yang, Thin Solid Films 515, (2007) 6094–6098.

[6] T. Dietl, Semicond. Sci. Technol. (2002) 17 (14), 377.

[7] M. DiDomenico, S.H.Wemple, J. Appl. Phys. 40, 720 (1969).

[8] S. H.Wemple and M.Didomenico, Phys. Rev. B, 3, (1971) 1338.

[9] M.Benhaliliba, C.E. Benouis, M.S. Aida, F. Yakuphanoglu , A. Sanchez Juarez, J. Sol-Gel Sci. Technol. (2010) 55:335–342 DOI 10.1007/s10971-010-2258-x.

[10] F. Yakuphanoglu, M. Sekerci, J.Mol.Struct.751 (2005)200.

[11] C. I. Oriaku, J. C. Osuwa, Journal of Ovonic Research Vol. 5, No. 6, December 2009, p. 213-218.

[12] M. R. Islam, J. Podder, Cryst. Res. Technol. 44, No. 3, 286 – 292 (2009) / DOI

10.1002/crat.200800326.

[13] Y. Caglar, S.Ilican M.Caglar, F.Yakuphanoglu, Spectrochim. Acta A67 (2007), 1113 – 1119.

[14] K.E. Peiponen, V. Lucarini, E.M. Vartiainen, and J.J. Saarinen, Eur. Phys. J. B 41, 61–65 (2004) DOI: 10.1140/epjb/e2004-00294-6.

[15] J. N. Hodgson, Optical Absorption and Dispersion in Solids, Chapman and Hall Ltd. 11 New Fetter Lane London EC4, (1970).

[16] Kurt E. Oughstun and Natalie A. Cartwright (C) (2003) OSA, Vol. 11, No. 13, Optics Express, 1541-1546.